



Chandra discovery of activity in the quiescent nuclear black hole of NGC821

A. Baldi¹, G. Fabbiano¹, S. Pellegrini², A. Siemiginowska¹, M. Elvis¹, A. Zezas¹, and J.C. McDowell¹

¹ *Harvard-Smithsonian Center for Astrophysics, 60 Garden St, Cambridge, MA 02138, USA* e-mail: abaldi@cfa.harvard.edu, gfabbiano@cfa.harvard.edu, aneta@cfa.harvard.edu, elvis@cfa.harvard.edu, azezas@cfa.harvard.edu, jcm@cfa.harvard.edu

² *Dipartimento di Astronomia, Università di Bologna, via Ranzani 1, 40127 Bologna, Italy* e-mail: silvia.pellegrini@unibo.it

ABSTRACT

We report the results of the *Chandra* ACIS-S observations of the elliptical galaxy NGC 821, which harbors a supermassive nuclear black hole (of $3.5 \times 10^7 M_{\odot}$), but does not show sign of AGN activity. A small, $8.5''$ long (~ 1 kpc at the galaxy's distance of 23 Mpc), S-shaped, jet-like feature centered on the nucleus is detected in the 38 ksec ACIS-S integrated exposure of this region. The luminosity of this feature is $L_X \sim 2.6 \times 10^{39}$ ergs s^{-1} (0.3-10 keV), and its spectrum is hard (described by a power-law of $\Gamma = 1.8_{-0.6}^{+0.7}$; or by thermal emission with $kT > 2$ keV). We discuss two possibilities for the origin of this feature: (1) a low-luminosity X-ray jet, or (2) a hot shocked gas. In either case, it is a clear indication of nuclear activity, detectable only in the X-ray band. Steady spherical accretion of the mass losses from the central stellar cusp within the accretion radius, when coupled to a high radiative efficiency, already provides a power source exceeding the observed radiative losses from the nuclear region.

1. INTRODUCTION

We currently know that virtually all galaxies host supermassive black holes (SMBH) in their nuclei. High resolution observations of the nuclei of elliptical galaxies and bulges have established the presence of these SMBHs (e.g. Magorrian et al 1998). However the lack of detectable nuclear emission in most galaxies where a SMBH is present makes the question more puzzling. Although a few faint AGNs have been detected in X-rays (e.g. in the $L_X/L_E \sim 10^{-(6-7)}$ range, where L_E is the Eddington luminosity of the SMBH; Pellegrini et al. 2003), we still do not have a clear picture of what impedes the formation of a luminous AGN.

NGC 821 represents an example of such galaxies, hosting a SMBH and where no nuclear emission has been detected so far. It is an E6 galaxy located at a distance of

M_{BT}^0 (mag)	D (Mpc)	Diam.($''$) σ_o (km s $^{-1}$)	N_H (cm $^{-2}$)	L_X (erg s $^{-1}$) $L_{H\alpha}$ (erg s $^{-1}$)	M_\bullet ($10^7 M_\odot$)	ObsID	Date	$T_{exp.}$ (ks)
-20.71	23	2.6	6.2×10^{20}	$< 5 \times 10^{40,1}$	2.8-5.8 2	4408	Nov. 26, 2002	24.6
...	...	209 3	...	$< 1.3 \times 10^{38,4}$...	4006	Dec. 1, 2002	13.3

¹Beuing et al. 1999; ²Gebhardt et al. 2003, rescaled for the distance adopted here; ³Prugniel & Simien 1996; ⁴Ho et al. 2003.

Table 1. NGC 821: Properties and *Chandra* ACIS-S Observation Log. Unless otherwise noted, the galaxy properties are as listed in NED (NASA / IPAC Extragalactic Database).

Fig. 1. Left: True color image of the central region of NGC 821, unsmoothed. The cross and surrounding circle represent the 2MASS nuclear position and uncertainty, from NED. Right: A larger field image showing both the *wavdetect* source regions (yellow) and the spectral extraction regions for the ‘jet’ and the diffuse emission (light blue).

23 Mpc, where the ACIS resolution at the aim point corresponds to 55 pc. Prior to our *Chandra* observation, NGC 821 had been observed, but not detected, in X-rays with *ROSAT* ($< 5 \times 10^{40}$ erg s $^{-1}$; Beuing et al. 1999). This limit is $\sim 10^5$ times below the Eddington luminosity of the nucleus, based on the SMBH mass of $2.8 - 5.8 \times 10^7 M_\odot$ (Gebhardt et al. 2003). As reported in Ho et al. (2003), NGC 821 has not been detected in radio continuum nor in optical emission lines ($H\alpha$ and $H\beta$), and is a good example of quiescent SMBH. In this talk we report the results of the *Chandra* ACIS observation of NGC 821, that has led to the discovery of an S-shaped feature, suggestive of either a weak two-sided X-ray nuclear jet, or of hot shocked gas.

2. OBSERVATIONS AND DATA ANALYSIS

NGC 821 was observed with *Chandra* ACIS-S (PI: Fabbiano) on November 26, 2002 (ObsID: 4408) and on December 1, 2002 (ObsID: 4006) for a total exposure time of 38 ks. Table 1 is a summary of the relevant properties of NGC 821 and of the observing log.

2.1. X-ray image

From the dataset obtained merging the two observations, images were extracted in three spectral bands (Red = 0.5 - 1 keV; Green = 1 - 2 keV; Blue = 2 - 4 keV).

A high resolution ‘true-color’ image of the central region of NGC 821 is shown in fig. 1a, where the data are displayed at the original observed resolution, without smoothing. This figure shows clearly a north-south elongated, hard central feature, centered on the nucleus of NGC 821, at RA=02^h08^m21.14^s, Dec=+10^o59’41.7’’ (J2000, with uncertainty of 1.25’’; from the 2MASS survey, as reported in NED). The general form is suggestive of a two-sided bent jet, or S-shaped filament centered on the nucleus. This feature is approximately 8.5’’ long, corresponding to ~ 1 kpc at the distance of NGC 821.

2.2. Spatial analysis of the nuclear feature

In the central region shown in fig. 1a, there are four sources: the isolated point-like source at the north-east of the central complex (source NE), and three sources in the

central elongated emission region, identified by ellipses in fig. 1b, and named S1, S2 and S3, from north to south. To establish their spatial properties, we have compared their spatial distribution of counts with that of the on-axis image of the quasar GB 1508+5714 (Siemiginowska et al 2003a), which can be used as a good representation of the *Chandra* ACIS-S PSF. With a count rate of ~ 0.05 count s^{-1} , the image of GB 1508+5714 (ObsID 2241) is not affected by pile-up, and contains 5,300 counts within $2''$ of the centroid of the count distribution. From this image, we determine the ratio of counts within the $1''$ - $2''$ annulus to those in the central $1''$ radius circle to be $Ratio(\text{PSF}) = 0.043 \pm 0.001$ (1σ). The isolated NE source in this central field yields $Ratio(\text{NE}) = 0.057 \pm 0.054$ (from a total of 36 source counts), entirely consistent with that of our reference quasar, confirming that GB 1508+5714 gives a good representation of the PSF. Instead, the analogous ratios for the background-subtracted counts from S1, S2 and S3 demonstrate that the emission is extended in all cases. Using the *wavdetect* centroids, we obtain $Ratio(\text{S1}) = 0.81 \pm 0.26$, $Ratio(\text{S2}) = 0.94 \pm 0.27$, and $Ratio(\text{S3}) = 0.29 \pm 0.10$. The total number of source counts in the three cases are 56, 67, and 71, respectively, larger than for source NE. This comparison demonstrates that the spatial distributions of the source counts from S1 and S2 are definitely not consistent with the PSF. Therefore, these three central emission regions are clearly not point-like and cannot be explained with the serendipitous positioning of three luminous galaxian LMXBs in NGC 821.

Given that the central emission (S2) is not consistent with a point-source, we can only estimate a 3σ upper limit on the luminosity of a nuclear point-like AGN. A $1'' \times 1''$ (2×2 pixels) sliding cell over the entire area covered by the S-shaped feature (assuming as the background level the maximum value detected in the sliding cell) yields a 0.3-10 keV $L_X < 4.2 \times 10^{38} \text{erg s}^{-1}$ for a $\Gamma = 1.8$ power-law spectrum and Galactic N_H . This limit indicates that a central point-like AGN would have a luminosity not exceeding that of normal LMXBs.

2.3. Spectral analysis

Hardness ratios (HR1=M-S/M+S; HR2=H-M/H+M; where S=0.5-1 keV, M=1-2 keV, and H=2-4 keV) are plotted (with 1σ statistical errors) in fig. 2, and compared with power-law and Raymond-Smith emission models. The hardness ratios of the S1, S2, S3 regions are all consistent with hard emission, either a power-law spectrum with Γ between ~ 1 and ~ 2.2 , or thermal emission with $kT \sim 2 - 20$ keV. The diffuse X-ray emission of an elliptical galaxy is the combination of the soft emission of the hot ISM and of the hard emission of the population of LMXBs below our detection threshold (see e.g, Kim & Fabbiano 2003). In NGC 821 the hardness ratios of the diffuse emission are hard, suggesting a dominant LMXB component and little hot ISM.

A proper spectral analysis was possible only on the whole S-shaped feature and not on the individual S1, S2 and S3 sources. Therefore spectra were extracted both from the S-shaped feature (regions in fig. 1b) and the surrounding diffuse emission (within a $20''$ radius)

With XSPEC, we fitted the data in the 0.3-10 keV energy range, rebinned at $N > 15$ counts per energy bin. For the S-shaped feature we adopted an absorbed power-law model (XSPEC model: *wabs(wabs(pow))*), with N_H consisting of both a Galactic and an intrinsic component. The results of the fits are listed in Table 2, with 90% errors on one significant parameter. The S-shaped emission is well fitted with a power-law spectrum with $\Gamma \sim 1.8$, typical of AGN spectra, although the uncertainties are large.

For the diffuse emission, following e.g. Kim & Fabbiano (2003), an optically thin thermal component ($Z = 0.3$) was added to the power-law model (XSPEC model:

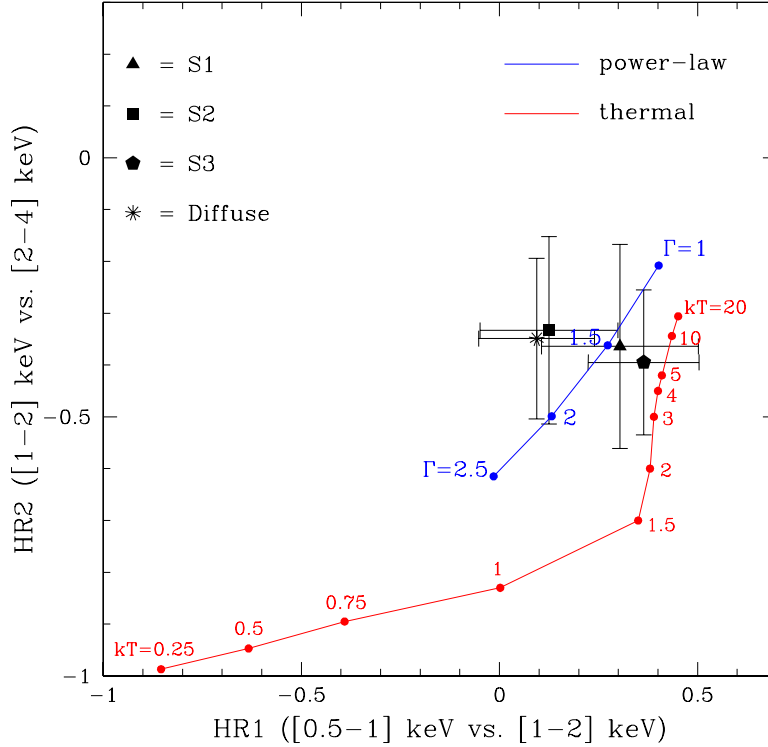


Fig. 2. X-ray colour-colour diagram of ‘jet’ and diffuse emission regions. Typical hardness ratios for a power-law model ($\Gamma = 1 - 2.5$) are plotted in blue. Typical hardness ratios for a thermal model ($kT = 0.25 - 20$ keV) are plotted in red. Galactic line-of-sight absorption ($N_H = 6.4 \times 10^{20} \text{cm}^{-2}$) is assumed in both models.

	Net Counts (0.3-10 keV)	χ^2/dof	N_H ($\times 10^{21} \text{cm}^{-2}$)	kT (keV)	Γ	$L_X(0.3 - 10 \text{ keV})$ (erg s^{-1})
S-shaped	141	6.7/5	$1.41^{+1.84}_{-1.41}$...	$1.82^{+0.71}_{-0.56}$	$2.6 \pm 0.5 \times 10^{39}$
...	...	6.5/5	$0.75^{+2.34}_{-0.75}$	$5.14^{+50.00}_{-2.99}$...	$1.9^{+1.4}_{-0.4} \times 10^{39}$
Diffuse	174	6.5/10	< 9.00	$0.46^{+0.33}_{-0.25}$	$1.27^{+1.13}_{-0.68}$	$3.5 \pm 0.6 \times 10^{39}$
Thermal	$3.4 \pm 0.1 \times 10^{38}$

Table 2. Results of Spectral Fits

$wabs(wabs(apec+pow))$). The diffuse emission spectrum (see Table 2) is consistent with a hot gas with a temperature $kT \sim 0.5$ keV, or cooler, typical of X-ray-faint early-type galaxy halos (e.g. Pellegrini & Fabbiano 1994). The power-law component is needed to obtain an acceptable fit for the diffuse emission, as clearly suggested by fig. 2, in agreement with the presence of an unresolved LMXB population.

Table 2 also lists the best-fit unabsorbed luminosities for the S-shaped feature, the total diffuse emission and the thermal component of the diffuse emission. The latter is only 10% of the total diffuse emission, indicating that NGC 821 is singularly devoided of hot ISM.

More details on data reduction and analysis can be found in Fabbiano et al. (2004).

3. DISCUSSION

Our observations fail to detect a point-like source at the nucleus, down to a 3σ limit of $L_X(0.3 - 10 \text{ keV}) < 4.2 \times 10^{38} \text{ erg s}^{-1}$, ~ 100 times fainter than the ROSAT limit (see Table 1). The nucleus is not detected in the FIR or in H_2 (Georgakakis et al. 2001) arguing against a strongly obscured AGN (and against a nuclear starburst). There is also no sign of strong intrinsic absorbing column in the X-rays (see Table 2). The general AGN ‘quiescent state’ is also supported by the lack of radio continuum and optical line emission (Ho et al. 2003). We detect instead an elongated ($\sim 1 \text{ kpc}$), possibly bent, emission feature, strongly suggestive of a two-sided X-ray jet or S-shaped filament, with a hard spectrum consistent with a $\Gamma \sim 1.8$ power-law or, if thermal, $kT > 2 \text{ keV}$. The X-ray luminosity of this feature is $\sim 1.9 - 2.6 \times 10^{39} \text{ ergs s}^{-1}$, corresponding to $\sim 5 \times 10^{-7}$ of the Eddington luminosity of the SMBH.

3.1. Is a jet directly emitting the hard X-rays?

The S-shaped, hard emission centered on the nucleus of NGC 821 could be a two-sided nuclear jet, as in radio galaxies. The spectral power-law slope of this emission has large uncertainties (Table 2), but is consistent with the X-ray spectra of other jets (Siemiginowska et al. 2003b; Sambruna et al 2004). However, unlike other extragalactic X-ray jets seen in luminous AGNs, where $L_X(\text{jet})/L_X(\text{AGN}) \sim 1-15\%$, this ‘jet’ has no associated core X-ray source, implying $L_X(\text{jet})/L_X(\text{AGN}) > 6$. However, the NGC 821 ‘jet’ could be similar to the somewhat steeper spectrum ($\Gamma \sim 2.3$) M87 jet (Wilson & Yang 2002), where the nuclear point-like AGN is fainter compared with the jet ($L_X(\text{jet})/L_X(\text{AGN}) \sim 2$). The 0.5 kpc (one-sided) scale of the NGC 821 ‘jet’ is also similar to the $\sim 1.5 \text{ kpc}$ of the M 87 jet, while most radio/X-ray jets extend over much larger distances, up to 300 kpc (Siemiginowska et al. 2003b).

Synchrotron emission is plausible to be the emission mechanism responsible for the S-shaped emission of NGC 821, in the jet hypothesis: $\alpha_{\text{radio-X}} \leq 0.7$ (estimated from the radio flux limit of 0.5 mJy at 5 GHz and the X-ray flux at 1 keV); this $\alpha_{\text{radio-X}}$ is consistent with the X-ray slope, and is typical of the synchrotron slope observed in radio lobes (Peterson 1997). A radio detection not far below the current limit is expected if synchrotron radiation produces the S-shaped emission at the center of NGC 821.

However $\alpha_{\text{radio-X}} \leq 0.7$ is also consistent with the values of $\alpha_{\text{radio-X}}=0.7-0.8$ reported for knots in powerful jets by Sambruna et al. (2004) who favor an Inverse Compton origin for the X-ray flux for most of the jet knots, based on the X-ray fluxes lying above an extrapolation of the radio-optical slope ($\alpha_{RO} > \alpha_{OX}$). The seed photons for Comptonization could be either from the synchrotron photons within the jet (the ‘self-Compton’ case) or could be the external to the jet photon field. In the self-Compton process the ratio of the synchrotron to Inverse Compton luminosities is given by the ratio of energy densities of the magnetic to the synchrotron radiation field. In equipartition both luminosities are of the same order, and since the observed X-ray luminosity is a factor of at least 10^3 higher than the radio upper limit, the self-Compton case is excluded.

External Comptonization is also ruled out: Felten & Morrison (1966, eq.47) showed that $I_S/I_C = U_B/U_{ph}(\nu_C/\nu_S)^{(3-m)/2}$. Here I_S and I_C are intensities of synchrotron and inverse Compton emission, U_B is the energy density of magnetic field, U_{ph} the energy density of the external photon field, ν_C/ν_S is the ratio between the frequency of the Compton scattered photon and the frequency of the synchrotron photon, m is the power law index of the electron distribution, which is linked to the spectral index, α_s of the synchrotron emission so $m = 1 - 2\alpha_s$. The quantities above can be easily measured from the X-ray luminosity, the starlight from the central cusp of NGC 821 (Gebhardt et al. 2003), and the 0.5 mJy flux limit at 5 GHz. Considering the radial dependence of the optical photon field, we obtain a maximum predicted Inverse Compton emission due to scattering of the starlight ranging from $3.7 \times 10^{36} \text{ erg s}^{-1}$ at 1 pc galactocentric radius, to $7.9 \times 10^{35} \text{ erg s}^{-1}$ at 500 pc (the maximum jet extension). We conclude that Inverse Compton radiation would be a small contribution to the X-ray emission, suggesting that synchrotron may be the dominant emission mechanism if the S-shape feature is indeed a jet.

3.2. Is hot gas responsible for the hard emission?

If the origin of the hard S-shaped emission is thermal, the most likely scenario, suggested by analogies with another galaxy, leads to the presence of shocks in the ISM, resulting from an outburst of nuclear activity, as in the case of NGC 4636 (Jones et al 2002). The hot ‘arms’ of this galaxy, a giant elliptical in Virgo with no reported nuclear activity or jets, suggest an interesting analogy with the S-shaped feature of NGC 821. These arms, having a larger spatial scale (8 kpc) and a lower temperature ($\sim 0.5 - 0.7$ keV) than the S-shaped feature of NGC 821, are two symmetric features crossing the galaxy center, discovered in the *Chandra* ACIS data of NGC 4636. The NGC 4636 arms are accompanied by a temperature increase with respect to the surrounding hot ISM, which led to the suggestion by Jones et al. of shock heating of the ISM caused by a nuclear outburst. As discussed in § 2.3, the S-shaped feature of NGC 821 could similarly be hotter than its surroundings. Assuming a temperature of $kT=3$ keV for this feature, close to the lower limit suggested by our spectral fit (Table 2), we obtain a density $n = 8.59_{-1.07}^{+1.06} \text{ cm}^{-3}$ (errors at 90%). Using the best-fit value (and a temperature of 3 keV), we obtain a thermal pressure exceeding by a factor of ~ 14 that quoted in §3.1 for the surrounding hot ISM, suggesting a non-equilibrium situation, if only thermal pressures are involved. However, given the uncertainties in both T and n , the thermal pressures of both S-shaped feature and surrounding ISM could be similar. It is clear that deeper *Chandra* observations are needed to better constrain the energetics of this feature.

3.3. Is accretion present?

Whether it is a jet or hot shocked gas, the S-shaped feature of NGC 821 requires a considerable energy input, an obvious source of which is accretion onto the nuclear SMBH. Taking at face value the indication of the two-component fit of the circum-nuclear diffuse emission, which is consistent with the presence of a $kT \sim 0.5$ keV thermal component, we can estimate the nuclear accretion rate, in the steady spherical accretion scenario of Bondi (1952). This estimate is rough, because the gravitational capture radius (which depends on the gas temperature and on the mass of the SMBH; see the textbook by Frank, King & Raine 2002) is $r_{acc} \sim 3 - 23$ pc in our case, smaller than the physical resolution of the image (55 pc, Table 1). Based on the circum-nuclear gas temperature and

density, that we estimate from the emission measure of the diffuse thermal component to be $n = 4.1_{-1.5}^{+10.9} \times 10^{-3} \text{cm}^{-3}$, the Bondi mass accretion rate (also following Frank, King & Raine 2002) is $\dot{M}_{acc} = 1.1 \times 10^{-7} - 2.0 \times 10^{-5} M_{\odot} \text{yr}^{-1}$, including again all the uncertainties in the SMBH mass, kT and n . The corresponding luminosity is $L_{acc} = 6.2 \times 10^{38} - 1.1 \times 10^{41} \text{ergs s}^{-1}$, with the customary assumption of 10% accretion efficiency. The luminosity of the S-shaped feature is within this range, therefore in principle it could be explained by Bondi accretion of the hot ISM.

However, since the hot ISM is the thermalized integrated result of the stellar mass losses, as a minimum one expects the total stellar mass loss rate \dot{M}_{\star} within r_{acc} to be accreted (there may also be gas inflowing from outside r_{acc}). \dot{M}_{\star} can easily be obtained from the luminosity density profile recovered from HST data for the central galaxy region (Gebhardt et al. 2003). Using a conversion factor from luminosity to mass loss rate for an old stellar population at the present epoch (e.g., Ciotti et al. 1991), this leads to $\dot{M}_{\star} = 9.8 \times 10^{-6}$ and $2.6 \times 10^{-4} M_{\odot} \text{yr}^{-1}$, for the two extreme values of r_{acc} . These \dot{M}_{\star} values are respectively a factor of ~ 90 and ~ 13 larger than the \dot{M}_{acc} values derived above for the same r_{acc} . Given that this estimate of \dot{M}_{\star} is quite robust, we must conclude that either the derivation of \dot{M}_{acc} above is inaccurate, or the gas is not steadily inflowing within r_{acc} . The former possibility cannot be excluded with the present data, since in our calculation of \dot{M}_{acc} we used a density n value that is an average measured over a region extending much farther out than r_{acc} ; $n(r_{acc})$ is likely to be significantly higher than this average (e.g., a factor of ~ 30 times higher, for a $n \propto r^{-0.9}$ profile).

Assuming that it is just the stellar mass loss rate within r_{acc} that is steadily accreted, accretion luminosities > 20 times larger than the observed L_X of the hard emission are recovered (from $L_{acc} = 0.1 \dot{M}_{\star} c^2$). Therefore the possible scenarios for NGC 821 are: (a) accretion occurs but with low radiative efficiency; (b) accretion sustains a jet (this can be coupled again to a low radiative efficiency), whose total power is of the order of L_{acc} , as in the modeling for IC 1459 (Fabbiano et al. 2003) and M87 (Di Matteo et al. 2003); (c) accretion is unsteady and therefore the hot ISM in the nuclear region needs not be inflowing (Siemiginowska et al 1996; Janiuk et al 2004). In this case the feedback from the central SMBH can be either radiative (Ciotti & Ostriker 2001) or mechanical (Omma et al. 2004) and make accretion undergo activity cycles: while active, the central engine heats the surrounding ISM, so that radiative cooling – and accretion – are offset; then the central engine turns off, until the ISM starts cooling again and accretion resumes. NGC 821 may be in a stage of such a cycle when a nuclear outburst has recently occurred. Note that the accretion luminosity that is radiatively absorbed by the ISM during an outburst (Ciotti & Ostriker 2001) largely exceeds the hard thermal emission observed at the center of NGC 821.

The presence of the central S-shaped feature that is *hotter* than the surrounding gas is uncontroversial evidence that central heating is at work, and therefore some type of feedback from the SMBH is occurring. The unsteady scenario seems promising to fit adequately the case of NGC821, also because this galaxy is clearly hot gas poor, as if recently swept by an outburst-driven wind. From our ACIS-S data we estimate an upper limit of $\sim 4 \times 10^6 M_{\odot}$ on the amount of hot ISM, many orders of magnitude smaller than for hot gas rich ellipticals (see Fabbiano 1989).

Acknowledgements. We thank the *Chandra* X-ray Center DS and SDS teams for their efforts in reducing the data and developing the software used for the data reduction (SDP) and analysis (CIAO). We have used the NASA funded services NED and ADS, and browsed the Hubble archive. This work was supported by NASA contract NAS 8–39073 (CXC) and NASA grant GO3-4133X

REFERENCES

- Beuing, J., Dbereiner, S., Bhringer, H. & Bender, R. 1999, MNRAS, 302, 209
- Bondi, H. 1952, MNRAS, 112, 195
- Ciotti, L., Pellegrini, S., Renzini, A. & D'Ercole, A. 1991, ApJ, 376, 380
- Ciotti, L. & Ostriker, J. P. 2001, ApJ, 551, 131
- Di Matteo, T., Allen, S. W., Fabian, A. C., Wilson, A. S. & Young, A. J. 2003 ApJ, 582, 133
- Fabbiano, G. 1989, ARAA, 27, 87
- Fabbiano, G. et al. 2003, ApJ, 588, 175
- Fabbiano, G. et al. 2004, Astro-ph 0405358, ApJ submitted
- Felten, J. E. & Morrison, P. 1966 ApJ, 146, 686
- Frank, J., King, A. & Raine, D. J. 2002 *Accretion Power in Astrophysics: Third Edition*, [Cambridge: Cambridge University Press]
- Gebhardt, K. et al. 2003, ApJ, 583, 92
- Georgakakis, A., Hopkins, A. M., Caulton, A., Wiklind, T., Terlevich, A. I. & Forbes, D. A. 2001, MNRAS, 326, 1431
- Ho, L. C., Filippenko, A. V., & Sargent, W. L. W. 2003, ApJ, 583, 159
- Janiuk, A., Czerny, B., Siemiginowska, A. & Szczerba, R. 2004, ApJ, 602, 595
- Jones, C. et al. 2002, ApJ Letters, 567, L115
- Kim, D.-W. & Fabbiano, G. 2003 ApJ, 586, 826
- Magorrian, J. et al. 1998, AJ, 115, 2285
- Omma, H., Binney, J., Bryan, G. & Slyz, A. 2004, MNRAS, 348, 1105
- Pellegrini S., & Fabbiano G. 1994, ApJ, 429, 105
- Pellegrini, S., Baldi, A., Fabbiano, G. & Kim, D.-W. 2003, ApJ, 597, 175
- Peterson B.M., 1997, *An Introduction to Active Galactic Nuclei* [Cambridge: Cambridge University Press].
- Prugniel, P & Simien, F. 1996 A&A, 309, 749
- Sambruna R.M. et al. 2004, ApJ in press. astro-ph/0401475.
- Siemiginowska, A., Czerny, B. & Kostyunin, V. 1996, ApJ, 458, 491
- Siemiginowska, A., Smith, R. K., Aldcroft, T. L., Schwartz, D. A., Paerels, F., & Petric, A. O. 2003a, ApJ, 598, L15
- Siemiginowska, A. et al. 2003b, ApJ, 595, 643.
- Wilson A.S., & Yang Y., 2002, ApJ, 568, 133

This figure "fig1a.jpg" is available in "jpg" format from:

<http://arxiv.org/ps/astro-ph/0410169v1>

This figure "fig1b.jpg" is available in "jpg" format from:

<http://arxiv.org/ps/astro-ph/0410169v1>